Chemistry & Biology
Article

Crystal Structure of the OXA-48 β-Lactamase Reveals Mechanistic Diversity among Class D Carbapenemases

Jean-Denis Docquier,[1] Vito Calderone,[2,3] Filomena De Luca,[1] Manuela Benvenuti,[2] Francesco Giuliani,[1] Luca Bellucci,[4] Andrea Tafi,[4] Patrice Nordmann,[5] Maurizio Botta,[4] Gian Maria Rossolini,[1] and Stefano Mangani[2,3,*]
[1]Dipartimento di Biologia Molecolare, Sezione di Microbiologia, Università di Siena, Siena I-53100, Italy
[2]Dipartimento di Chimica, Università di Siena, Siena, I-53100, Italy
[3]Magnetic Resonance Center CERM, Università di Firenze, Sesto Fiorentino I-50019, Italy
[4]Dipartimento Farmaco-Chimico-Tecnologico, Università di Siena, Siena I-53100, Italy
[5]Service de Bactériologie-Virologie, Hôpital de Bicêtre, Université Paris XI, Le Kremlin-Bicêtre, Paris F-94275, France
*Correspondence: mangani@unisi.it
DOI 10.1016/j.chembiol.2009.04.010

SUMMARY

Carbapenem-hydrolyzing class D β-lactamases (CHDLs) are enzymes found in important Gram-negative pathogens (mainly *Acinetobacter baumannii* and *Enterobacteriaceae*) that confer resistance to β-lactam antibiotics, and notably carbapenems. The crystal structure of the OXA-48 carbapenemase was determined at pH 7.5 and at a resolution of 1.9 Å. Surprisingly, and by contrast with OXA-24, the only other CHDL of known crystal structure, the structure of OXA-48 was similar to OXA-10, an enzyme devoid of carbapenemase activity, indicating that the hydrolysis of these compounds could depend on subtle changes in the active site region. Moreover, the active site groove of OXA-48 was different from that of OXA-24 in shape, dimensions, and charge distribution. Molecular dynamics pointed to the functional relevance of residues located in or close to the β5–β6 loop and allowed us to propose a mechanism for carbapenem hydrolysis by OXA-48.

INTRODUCTION

Class D β-lactamases (DBLs) are bacterial enzymes involved in resistance to β-lactam antibiotics. Until recently, they were considered of low clinical relevance due to their narrow substrate specificity (mostly restricted to penicillins and narrow-spectrum cephalosporins) and overall low prevalence among bacterial pathogens (Naas and Nordmann, 1999). The emergence of DBLs able to hydrolyze oxyimino-cephalosporins and carbapenems (i.e., the most potent and recent β-lactams) has changed this view, and these enzymes are now considered emerging resistance determinants of notable clinical importance (Poirel et al., 2007; Queenan and Bush, 2007). Carbapenem-hydrolyzing class D β-lactamases (CHDLs), in particular, can confer resistance to carbapenems in major Gram-negative pathogens such as *Acinetobacter* spp. and *Enterobacteriaceae*, and represent a formidable threat, as carbapenems are among the very few therapeutic options left for the treatment of multidrug-resistant strains of those species (Poirel et al., 2007; Queenan and Bush, 2007; Walther-Rasmussen and Hoiby, 2006).

The X-ray structures of two different lineages of DBLs, OXA-10 (Paetzel et al., 2000; Maveyraud et al., 2000) and OXA-1 (Sun et al., 2003), have revealed an overall conserved molecular fold in comparison with other serine-β-lactamases, but also peculiar features with mechanistic implications, namely: (i) an extended substrate-binding cleft, due to a more compact conformation of the Ω loop and to a shorter size of additional loops; and (ii) carbamylation of the invariant Lys residue found in the SxxK conserved motif. This posttranslational modification is essential to the catalytic process of DBLs by activation of the active-site serine, which promotes its acylation by the β-lactam substrate, and by subsequent activation of a water molecule essential to deacylation of the acyl-enzyme complex (Golemi et al., 2001; Li et al., 2005). The determination of the structure of OXA-13 (a close allelic variant of OXA-10) in complex with meropenem, a carbapenem antibiotic, provided the first insights into the interaction of DBLs with carbapenem substrates, showing that formation of the acyl-enzyme species is associated to a conformational change in the active site, which results in positioning of the catalytic water molecule at too far a distance from the acyl carbonyl group of the substrate. As a consequence, meropenem is poorly deacylated, and this accounts for enzyme inhibition (Pernot et al., 2001). Most recently, the crystal structure of a CHDL, OXA-24, has been solved, and structural analysis plus site-directed mutagenesis experiments have provided important insights into the mechanism by which the enzyme interacts with carbapenem substrates (Santillana et al., 2007). In particular, the presence of a hydrophobic barrier that restricts the access to the active site cleft, contributed by the side chains of two residues (Tyr-112 and Met-223), would account for the specificity of OXA-24 for carbapenems. However, the mechanism that allows efficient carbapenem hydrolysis by OXA-24 in comparison with other DBLs could not be explained. Moreover, the structure of OXA-24 has been determined at pH 4.5, i.e., a "nonphysiological" condition different from that at which the enzyme activity has been investigated (Santillana et al., 2007).

This work describes the crystal structure and the properties of OXA-48, a CHDL that is highly divergent from DBLs of known

three-dimensional structure, including OXA-24. OXA-48 was originally identified in a carbapenem-resistant clinical isolate of *Klebsiella pneumoniae*, in which the enzyme contributed to the carbapenem-resistant phenotype (Poirel et al., 2004). Recently, the spread of carbapenem-resistant strains producing this enzyme has been reported in different countries and suggests a potential for dissemination in the clinical setting (Aktas et al., 2008; Gülmez et al., 2008; Carrer et al., 2008; Cuzon et al., 2008). To probe the evolution of carbapenem hydrolysis among class D β-lactamases, we obtained original structural data and investigated the OXA-48 structure-activity relationships by molecular dynamics. This approach provided additional and original insights into the mechanisms of carbapenem hydrolysis by DBLs.

RESULTS

Biochemical and Biophysical Features of OXA-48

OXA-48 was overproduced in *Escherichia coli* in the native form and purified (>99%) by three chromatographic steps. The mass of the purified protein, determined by ESI-MS, was 28,145 ± 2 Da, confirming that, as predicted (Bendtsen et al., 2004), the mature protein is obtained after removal of a 22-amino acid leader peptide. The apparent M_r of the protein in solution, determined by size-exclusion chromatography, was 50 ± 6 kDa, suggesting a dimeric structure for the native enzyme, similar to some DBLs (e.g., OXA-10 [Paetzel et al., 2000; Maveyraud et al., 2000], OXA-13 [Pernot et al., 2001], OXA-2 [Dale and Smith, 1976], OXA-29 [Franceschini et al., 2001], and OXA-46 [Giuliani et al., 2005]) but different from others, which are monomeric (e. g. OXA-1 [Sun et al., 2003], OXA-24 [Santillana et al., 2007], and OXA-85 [Voha et al., 2006]). The apparent M_r of OXA-48 in solution was not affected by the addition of 5 mM EDTA in the elution buffer, showing that, unlike for OXA-10 (Danel et al., 2001; Paetzel et al., 2000), dimerization was not dependent on divalent cations.

Kinetic analysis confirmed the substrate specificity of OXA-48, which includes carbapenem substrates, with a strong preference for imipenem and panipenem compared with the 1-β-methyl-carbapenems meropenem and ertapenem. The differences in catalytic efficiency (approximately 100-fold) were due to a lower turnover rate with 1-β-methyl-carbapenems and, with ertapenem, also to a reduced affinity (Table 1). Interestingly, the kinetic behavior of OXA-48 with carbapenems was quite different from that of the OXA-24, which exhibits similar turnover rates for imipenem and meropenem and is overall more active on meropenem due to a much higher affinity for that substrate (Santillana et al., 2007). Another notable difference between OXA-48 and OXA-24 concerns the behavior with oxacillin, which for OXA-48 is one of the best substrates, whereas for OXA-24 is a very poor substrate (Santillana et al., 2007).

Table 1. Kinetic Parameters of Oxa-48 with Representative β-Lactam Substrates

Substrate	k_{cat} (s^{-1})	K_m (μM)	k_{cat}/K_m ($M^{-1}\cdot s^{-1}$)
Oxacillin	130	95	1.4×10^6
Ampicillin	955	395	2.4×10^6
Temocillin	0.3	45	6.6×10^3
Nitrocefin	940	120	7.7×10^6
Cephalothin[a]	44	195	2.3×10^5
Cefoxitin	>0.05	>200	2.6×10^2
Cefotaxime	>9	>900	1.0×10^4
Ceftazidime[b]	N.H.	-	-
Cefepime	>0.6	>550	1.1×10^3
Imipenem	4.8	13	3.7×10^5
Meropenem	0.07	11	6.2×10^3
Ertapenem	0.13	100	1.3×10^3
Panipenem	1.4	14	1.0×10^5
Faropenem	0.038	13	2.9×10^3

Values calculated on the basis of three independent experiments; SDs were below 10%.

[a] Biphasic kinetics were observed with this substrate. However, the rapid establishment of the steady state did not allow the measurement of initial rate kinetic parameters.

[b] Hydrolysis of ceftazidime could not be detected with concentrations of substrate and enzymes up to 500 μM and 400 nM, respectively.

Protein Fold and Quaternary Structure

The crystal structure of OXA-48 (PDB code 3HBR), solved by molecular replacement using OXA-10 as model and refined to 1.9 Å resolution (Table 2), consists of two independent OXA-48 dimers contained in the crystal asymmetric unit.

Despite a remarkable sequence divergence (25%–48% identical residues; see Figure S1 available online), the OXA-48 tertiary structure is very similar to that of other DBLs of known crystallographic structure (Figure 1). Rmsd values on common Cα atoms ranges from 1.02 to 1.40 Å, with OXA-24 and OXA-1, respectively. Small differences are located mainly in the loops connecting secondary structure elements, which may vary in length and orientation (Figure 1B). The disulfide bridge between Cys-44 and Cys-57 that links β2 to β3 in OXA-10 and OXA-13 is absent in OXA-48, where these residues are replaced by Trp-47 and Gly-54. Other conformational differences between OXA-48 and OXA-10, OXA-13 and OXA-1 are present in (i) the β4–β5 loop, (ii) the β7-α10 loop, and (iii) the strands β5 and β6, which are shorter overall. As a consequence, the orientation of the β5–β6 loop in OXA-48 (similar to OXA-24) differs in length and orientation from that observed in other DBLs. The Ω loop in OXA-48 adopts the same conformation as that of other DBLs except OXA-1, where it apparently shows a different organization which reflects the insertion of six residues. In addition, the α3–α4 loop containing the conserved Trp-95 residue, which appeared to be disordered in some other DBL structures (Paetzel et al., 2000; Maveyraud et al., 2000), was clearly visible in all OXA-48 subunits and contained several interactions that might contribute to its stabilization. In particular, His-109 is H-bonded to Thr-104 backbone carbonyl and to the Thr-113 side chain hydroxyl group, as already observed in the OXA-1 structure (Sun et al., 2003).

In contrast with OXA-1 and OXA-24, the quaternary structure of OXA-48 is dimeric, in agreement with the results of size-exclusion chromatography, and shows a noncrystallographic pseudo 2-fold axis (see Supplemental Data; Figure S2). The OXA-48 dimer formation buries about 930 $Å^2$ of monomer surface, which is smaller by 200 $Å^2$ than that buried in OXA-10 (1130 $Å^2$), suggesting a weaker dimer-dimer interface. The dimer is obtained

Table 2. Crystallographic Data Processing and Refinement Statistics

Data collection statistics (λ = 0.934 Å)	
Space group	$P2_1$ (Z = 4)
Cell dimensions (Å,°)	a = 63.70; b = 107.18; c = 80.79; β = 111.04
Resolution (Å)	32.2−1.9 (2.0−1.9)
Total reflections	457,879 (67,749)
Unique reflections	78,362 (11,507)
Completeness	99.0 (99.4)
R_{sym} (%)	10.04 (17.6)
Multiplicity	5.8 (5.9)
I/I)	5.3 (3.6)
Refinement statistics	
Resolution range (Å)	30.51−1. 9
R_{cryst} (%)	21.69
R_{free} (%)	28.62
Protein atoms	7853
No. of reflections in $R_{free\ set}$, (%)	7101−9.0
Ethylene glycol molecules	4
Water molecules	760
Mean B-factor protein ($Å^2$)	16.9
Mean B-factor solvent ($Å^2$)	26.9
Rmsd bond lengths (Å)	0.016
Rmsd bond angles (°)	1.61
Rmsd dihedrals (°)	6.51
Rmsd chiral volumes ($Å^3$)	0.115
Ramachandran plot statistics	
Residues in allowed regions	862, 99.4%
Residues in generously allowed regions	5, 0.6%
Residues in disallowed regions	0, 0.0%

by building an intermolecular β sheet that involves β6 from each subunit related by the noncrystallographic 2-fold axis. The intermolecular β-sheet formation is due to only two direct H-bonds and reinforced by several water-mediated H-bonds and salt bridges, as well as by some hydrophobic interactions.

Active Site

The active site of OXA-48 is located in a narrow crevice of ~5 × 10 × 20 Å (width, depth, length) between the two domains and closed at one end by Arg-214 (β5–β6 loop) and the facing Gln-124 (α5), and by Ile-102 (α3–α4 loop) and the facing Ser-244 (helix 3_{10}d) at the other end (Figure 2A). The active site of OXA-48 presents the three conserved motifs typical of DBLs (Figures 1A and 2A) and, as already observed in some other DBL structures, a carbamylated lysine residue (motif I Lys-73), clearly visible in the electron density maps of all independent subunits (Figure 3).

Comparison with other DBLs shows that the catalytically relevant residues Ser-70, Lys-73, and Arg-250 are spatially conserved. The so-called "oxyanion hole," delimited by the Ser-70 and Tyr-211 peptide nitrogens and apparently responsible of the tetrahedral oxyanion intermediate stabilization, is occupied in all subunits by a water molecule (Wat2; Figure 3). A striking feature of OXA-48 is the peculiar conformation adopted by the β5–β6 loop, which extends into the outer portion of the active site crevice, modifying its charge distribution and narrowing its width to 5.5 Å (distance between Gln-124 and Arg-214), with respect to the 8.2 Å width occurring in the corresponding part of the active site crevice of OXA-10 in which the same loop adopts an open conformation (Figures 2A and 2B; Paetzel et al., 2000; Maveyraud et al., 2000). This conformation might be promoted by the interaction of Arg-214 with the Ω loop Asp-159 residue. In this way, the β5–β6 loop defines a rather hydrophilic cavity where several crystallographic water molecules are found, which are located close to the substrate binding site and could reach the scissile acyl-enzyme bond to perform the nucleophilic attack leading to the deacylation step.

Structure-Function Comparison of OXA-48 and OXA-24

The comparison of the OXA-48 and OXA-24 crystal structures reveals few differences, represented by a shorter N-terminal α1 helix in OXA-48 and by the twist of the β sheet, which is more pronounced in OXA-24. Interestingly, the orientation and size of the β5–β6 loop is very similar in OXA-24 and OXA-48 (Figure 1B), suggesting its possible involvement in carbapenem hydrolysis. Notwithstanding this common feature, the functional properties of both enzymes are significantly different, as OXA-48 exhibits a preference for imipenem over meropenem and ertapenem, whereas OXA-24 apparently shows a strong preference for meropenem, although contrasting kinetic parameters have been reported in the literature for this enzyme (Santillana et al., 2007; Bou et al., 2000).

Comparison of the active site region of OXA-48 and OXA-24 reveals that the two cavities differ in shape, dimensions, and charge distribution. Figure 2C shows that the tunnel-like entrance of the active site present in OXA-24 (the Tyr-112-Met-223 hydrophobic barrier), taken as the structural determinant for the preference for the smaller carbapenem substrates versus the bulkier oxacillin (Santillana et al., 2007), is missing in OXA-48. This is consistent with the different behavior of the two enzymes toward oxacillin. A further difference exists in the loop β7-α10, which has bulkier residues and a different conformation in OXA-48 with respect to OXA-24, causing a narrower cleft in the region behind the OXA-24 Tyr-112-Met-223 barrier (OXA-48 Ile-102-Ser-244 distance of 7.65 Å compared with OXA-24 Tyr-112-Glu-254 distance of 11.05 Å).

Structural Motifs Relevant to Carbapenem Hydrolysis

The 3D structure comparison reveals that OXA-48 has closer similarity to OXA-10/13 than to OXA-24, while sharing the carbapenemase activity only with the latter enzyme. However, OXA-24 differs from OXA-10/13 in both activity and active site structure. Thus, the carbapenemase property of OXA-48 must depend on individual amino acid differences able to influence the reaction pathways for the different substrates.

Based on this assumption, a closer comparative analysis was carried out searching for minor differences in the active-site cavity of OXA-48 and OXA-10/13. This analysis came up with at least four residues, namely His-109, Thr-213, Arg-214, and Ser-244, which could be responsible for functional differences. In particular, His-109 provides interactions with Thr-104 and Thr-113, and could influence, by modifying the hydrogen

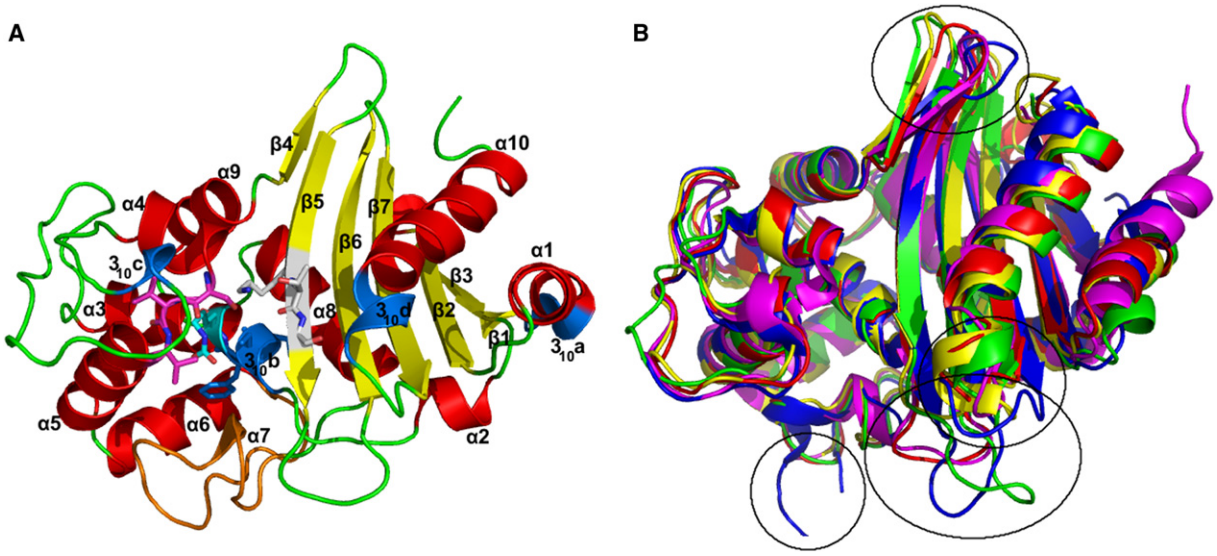

Figure 1. Tertiary Structure of OXA-48 and Comparison with Other DBL Structures

(A) Ribbon representation of an OXA-48 subunit, showing the secondary structure elements assigned as follows: β1: 26–28; 310a: 29–31; α1: 31–35; β2: 42–48; β3: 53–56; α2: 59–62; 310b: 69–72; α3: 73–82; 310c: 103–105; α4: 110-115; α5: 120–130; α6: 132–142; α7: 156–159; α8: 166–177; α9: 185–194; β4: 196–199; β5: 204–212; β6: 219–227; β7: 232–240; 310d: 244–246; α10: 245–260. α helices are shown in red; β strands in yellow and turns in green. The Ω loop is colored orange. The three DBL motifs are shown with the respective residues as sticks: motif I (containing the catalytic residues Ser-70, Thr-71, Phe-72, and carbamylated Lys-73), cyan; motif II (Ser-118, Val-119, and Val-120), magenta; motif III (Lys-208, Thr-209, and Gly-210), white.

(B) Least-squares superposition of representative members of the DBL family. The loops where different conformations are observed are framed as well as the catalytically relevant portions of the molecule. Color legend and PDB codes are as follows: OXA-48 (3HBR), red; OXA-1 (1M6K), blue; OXA-2 (1K38), yellow; OXA-10 (1K55), green; OXA-24 (2JC7), magenta.

bonding network, the dynamic behavior of the α3–α4 loop carrying the motif II residues; this is further supported by the fact that this loop is disordered in the crystal structure of native OXA-13 (1H5X), in which His-109 is replaced by a Leu (Pernot et al., 2001). Thr-213, Arg-214, and Ser-244 define the active cavity and are unique among all OXA structures. Arg-214 is also responsible for the typical closed conformation of the β5–β6 loop, due to a salt bridge formation with Asp-159 (Figure 3). In addition, OXA-24 does not bear any residue structurally equivalent to Ser-244, as the corresponding loop adopts a different conformation (Figure 1B).

MD Simulation with Carbapenem Adducts of OXA-48 and OXA-13

On the basis of the above results and in order to investigate the different behavior of two model DBLs toward carbapenem hydrolysis (inactivation versus deacylation), the acyl-enzyme complexes of OXA-13 and OXA-48 with meropenem were built on the basis of the meropenem-OXA-13 complex crystal structure (1H8Y) and subjected to a molecular dynamics (MD) simulation in explicit solvent (see Supplemental Data for details), using a carbamylated active site Lys in both enzymes. The starting point of the MD simulation was the relaxed OXA-48-meropenem

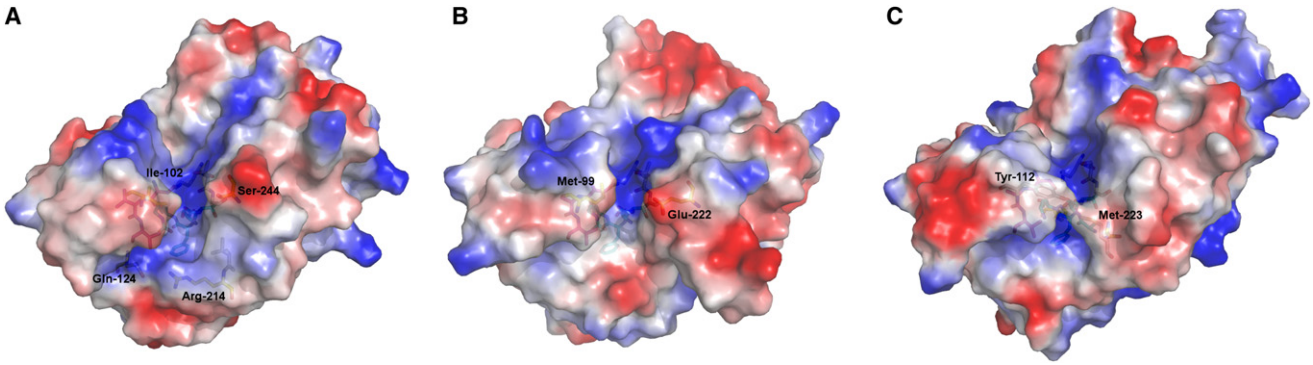

Figure 2. Comparison of the Surfaces and Electrostatic Potentials of OXA-48, OXA-10, and OXA-24

Surfaces of OXA-48 (A), OXA-10 (B), and OXA-24 (C) colored by electrostatic potential (blue, positive; red, negative) with the underlying stick model of motifs I–III (color coded as in Figure 1) and of the residues delimiting the active site cavity (yellow). The three figures have been taken approximately on the same orientation of the molecules.

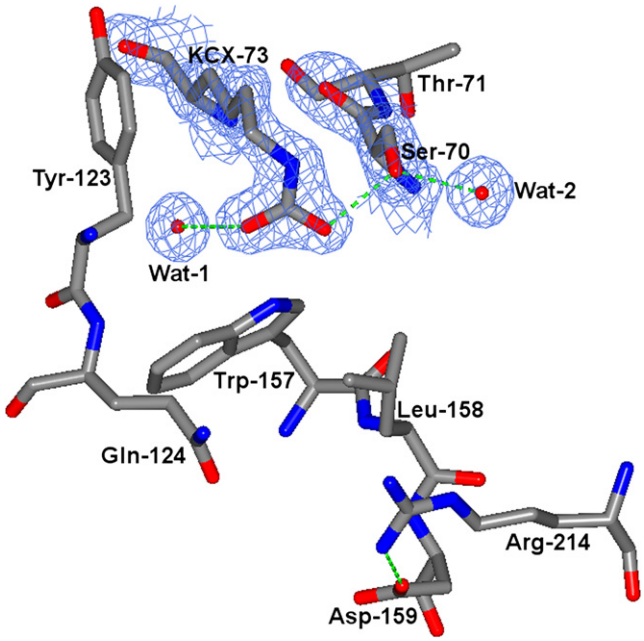

Figure 3. Active Site Region of OXA-48

The carbamylated side chain of the active site residue Lys-73 is shown together with nearby residues and water molecules. Superimposed is the 2Fo-Fc Fourier difference map calculated with phases from the final refined model and contoured at 1.5 σ level. The two water molecules present close to the catalytic residues are represented by red spheres of arbitrary radius.

acyl-enzyme, obtained by docking. In this structure, the substrate adopted an orientation similar to that of the meropenem-OXA-13 complex, with the meropenem carboxylate being involved in a salt bridge with Arg-250 and the 6-α-hydroxylethyl substituent located in a cavity defined by residues Lys-73 and Val-120 on one side, and Trp-105, Trp-157, Leu-158, Thr-213, and Arg-214 on the other (Figure 4). The methyl group of meropenem was pointing in the direction of Leu-158, while the hydroxyl group was more exposed to the solvent toward residue Val-120. A 10-ns MD simulation evidenced a recurring movement of the substrate hydroxyethyl moiety by a rotation of about 30 degrees around the bond connecting this group to the molecular scaffold. By this rearrangement, the substrate methyl group of the hydroxyethyl substituent was accommodated in a small cavity formed by the side chains of residues Leu-158 and Thr-213. Following the methyl movement, a water molecule previously lying in proximity of the carbamylated residue Lys-73 could approach the scissile bond at a distance of ~3.8 Å while forming a hydrogen-bond with the carbamyl group of Lys-73. With OXA-13, a similar rearrangement could only be observed once during the MD simulation, and for a shorter time than with OXA-48. These results are compatible with the much less favorable efficiency for deacylation step in OXA-13.

The above findings were confirmed by performing a mapping analysis of the catalytic region of OXA-48 and OXA-13 with the GRID method (Goodford, 1985) to search for sites within the catalytic region of both enzymes that could be complementary to the methyl group present in the 6-α-hydroxyethyl substituent of meropenem. Results of GRID calculations for OXA-48 (Figure S3) showed a 3 Å-long patch of hydrophobic interaction coming out from a small pocket formed by Thr-213 and Leu-67 and directed toward residue Leu-158. By contrast, a smaller region of favorable hydrophobic interaction was observed in OXA-13 (Figure S3). The larger interaction area of OXA-48 suggests both a more favorable interaction of the carbapenem methyl group with the cavity and its increased mobility, in comparison with OXA-13. Enthalpy estimations, performed on the MD trajectories by calculations of the average interaction energy between the substrate methyl group and the protein, confirmed GRID results yielding a lower mean energy value for OXA-13 than for OXA-48 (−0.9 versus −4.0 kcal/mol, respectively). The ensuing increased mobility of the 6-α-hydroxyethyl moiety of the bound meropenem that occurs in OXA-48 contributes to increase the probability of one of the water molecules to reach a location compatible with its activation to act as the nucleophile in the deacylation step of the reaction.

DISCUSSION

Despite the availability of structural information of DBLs, the factors responsible for the heterogeneity observed in their behavior toward carbapenems have not been yet unequivocally identified. Our results, critically compared with the data already available in the literature, allow us to view in a different perspective the mechanism of carbapenem hydrolysis by DBLs.

The active site Lys-73 of OXA-48 is carbamylated in all four independent subunits present in the crystal asymmetric unit and H-bonded by the carbamyl group to Ser-70 Oγ, to Trp-157 Nε, and to a water molecule deeply buried in the cavity (Figure 3). The same modification has been also observed in the crystal structures of OXA-1 and OXA-10 at pH 8.5, and experimental evidence is available indicating the involvement of carbamylation in the enzyme deacylation step (Golemi et al., 2001). For this reason and by contrast with OXA-24, whose structure has been determined at pH 4.5 and in which the active site lysine is not carbamylated, the present structure of OXA-48 (determined at 1.9 Å resolution and at pH 7.5) most likely corresponds to the structure of the active enzyme (the activity of OXA-48 is strongly decreased at pH 4.5; data not shown).

The sequence comparison of various DBLs shows that OXA-48 is closer to OXA-10 (45% identity), which is by contrast inhibited by carbapenems, than to OXA-24 (31%). This observation highlights the difficulty in predicting the carbapenem hydrolysis on the basis of the primary structure. Moreover, comparing the OXA-48 and OXA-24 crystal structures reveals that such predictions are also beyond the possibilities of structural analysis, as the "hydrophobic barrier" (Tyr-112, Met-223) over the active site of OXA-24 is definitely not a conserved motif distinctive of carbapenemase activity. The evidence is that the two different enzymes owe their carbapenemase properties to different structural motifs and active site shapes. The latter point provides a structural basis for the different functional properties of OXA-24 and OXA-48, i.e., their different catalytic properties toward carbapenems and oxacillin (see Table 1).

The computational studies performed on OXA-13 and OXA-48 complexes with meropenem provide interesting clues to understand the different behavior of the two enzymes toward carbapenems, and strongly support the concept that point mutations in the regions surrounding the catalytic residues Ser-70 and

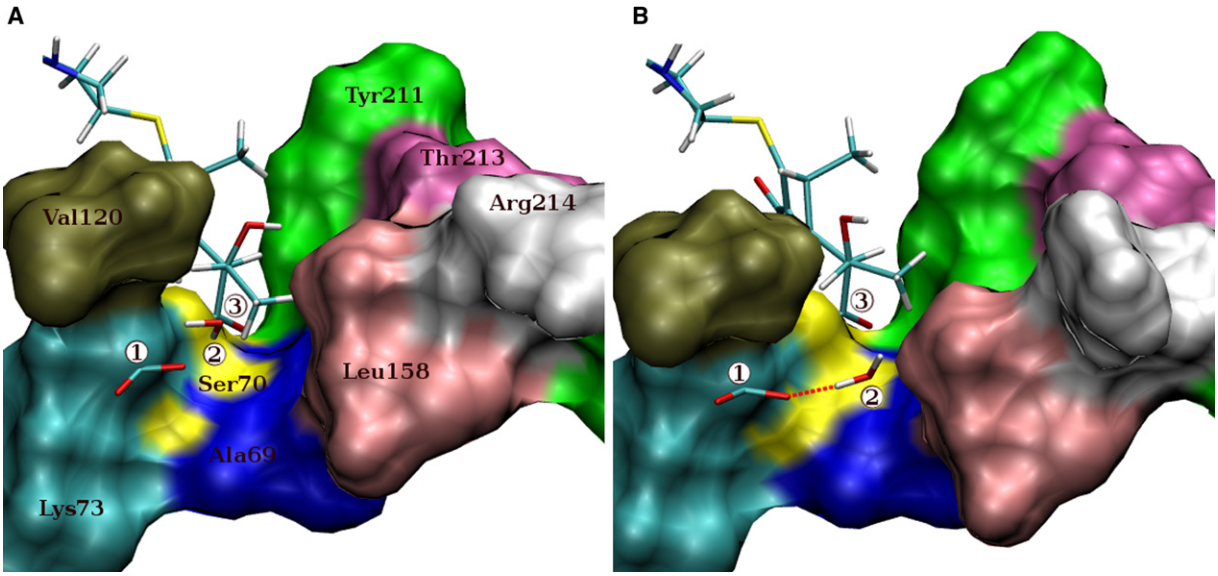

Figure 4. MD Snapshots of Meropenem (Stick Representation) Bound within the Active Site of OXA-48

Relevant residues of the active site are displayed in different colors as solvent accessible surface, and the carbamyl group of Lys-73 (cyan) is explicitly displayed as sticks (label 1). The water molecule involved in the deacylation step as described in the text is shown in stick representation (label 2) near Lys-73. The substrate acyl group bound to Ser-70 (yellow) is pointed out by label 3.

(A) Nonproductive geometry: the meropenem adopts a conformation in which the methyl group of the hydroxyethyl substituent points toward Leu-158 (pink) and the hydroxyl group is more exposed to the solvent. In this conformation the methyl group obstructs the access of water molecule 2 to the carbonyl carbon 3, which remains at ~6 Å apart from the scissile bond, thus corresponding to a nonproductive geometry.

(B) Productive geometry: the meropenem adopts a conformation in which the methyl group of the hydroxyethyl substituent is located within the niche formed by the side chains of residues Leu-158 (pink) and Thr-213 (magenta), and the hydroxyl group has moved closer to residue Val-120. In this conformation, water molecule 2 is hydrogen bonded to Lys-73 and is properly oriented to perform the nucleophilic attack on the carbonyl carbon (label 3).

Lys-73 lead to opposite fates for the meropenem molecule (accumulation of acyl-enzyme versus deacylation).

CHDLs represent a heterogeneous group of enzymes, and the availability of more crystal structures and functional data of these enzymes will tell whether the typical orientation of the β5–β6 loop and/or its amino acid composition is the key factor in carbapenem hydrolysis. Considering OXA-48 and OXA-24 as two different model CHDLs, it is now clear that they eventually acquire their carbapenemase activity through different evolutionary pathways, leading to different active site shapes. Interestingly, OXA-48 was able to acquire carbapenemase activity without losing the hydrolysis of oxacillin, typically the best substrate of OXA-type enzymes, which is poorly hydrolyzed by OXA-24, likely reflecting a more dramatic evolutionary trade-off in the latter.

The increasing clinical relevance of CHDLs underlines the need for new β-lactamase inhibitors that would restore the efficacy of the latest β-lactam agents. Considering the structural and mechanistic differences among CHDLs highlighted by the present work, this challenging area of drug discovery will need further structural and biochemical work to identify inhibitors potentially active on structurally different enzymes.

SIGNIFICANCE

In this work, we have determined the structure of the class D carbapenemase OXA-48, which is highly divergent from OXA-24, another carbapenemase whose structure was recently obtained. From both structural and functional standpoints, these two carbapenemases are strikingly different, indicating that different evolutionary strategies could lead to enzymes able to hydrolyze carbapenem antibiotics. More strikingly, the tunnel-like access found in OXA-24 is not found in OXA-48, indicating that this structural element is not required for carbapenem hydrolysis. A molecular dynamics approach was used to identify residues potentially involved in carbapenem hydrolysis and to propose a new catalytic mechanism of carbapenems by DBLs. According to our results, efficient hydrolysis of carbapenems would rely on the rotation of the substrate α-hydroxyethyl group promoted by the nature and conformation of residues located in or close to the β5–β6 loop, which subsequently allows the movement of the deacylating water molecule toward the acylated serine residue.

EXPERIMENTAL PROCEDURES

Bacterial Strains, Plasmids, and Culture Conditions

The recombinant plasmid pVT-1 was used as a source of the bla_{OXA-48} gene (Poirel et al., 2004). The bla_{OXA-48} ORF was subcloned into expression vector pET-9a (Novagen Inc., LaJolla, CA) to yield recombinant plasmid pET-OXA-48. *E. coli* MCT236(DE3) (kindly provided by Dr. Cristina Thaller) was used as the host for overproduction of the OXA-48 enzyme. β-lactamase production was carried out aerobically in Superbroth medium supplemented with 50 μg/ml kanamycin at 37°C.

Purification of OXA-48

Bacterial cells were collected by centrifugation, resuspended in 10 ml of 20 mM triethanolamine-H_2SO_4 buffer (pH 7.2) and disrupted using a Constant

Cell Disruption System (Constant System Ltd. Low March, Daventry, U.K). Cell debris were removed by centrifugation (10,000 × *g* for 60 min at 4°C), and the β-lactamase was purified from the clarified extract using two anion-exchange chromatographic separations followed by gel filtration step. This protocol reproducibly yielded approximately 30 mg of purified protein per liter of culture. The purity of the protein preparation was estimated to be >99% by SDS-PAGE analysis.

Characterization of OXA-48

Determination of kinetic parameters for various β-lactam substrates was carried out as previously reported (Giuliani et al., 2005) in 100 mM Tris-H_2SO_4 buffer supplemented with 300 mM K_2SO_4 (pH 7.0; buffer A) (Paetzel et al., 2000). The effect of EDTA on enzyme activity was determined after incubation of the enzyme for 20 min at 30°C with variable concentrations of EDTA in assay buffer A, using ampicillin as substrate. ESI-MS was carried out as described previously (Docquier et al., 2002). Apparent molecular weight in solution was determined by gel filtration chromatography as previously described (Docquier et al., 2003) using 0.4 mg of purified OXA-48 in buffer A. The effect of EDTA on the apparent M_r was investigated in buffer A supplemented with 10 mM EDTA.

Structure Determination and Refinement

OXA-48 crystals were obtained by the sitting-drop setup using 0.1 M HEPES buffer at pH 7.5, 10% PEG 4000, 8% 1-butanol. Several datasets from these crystals have been collected at 100 K on the ID14-1 beamline at the European Synchrotron Radiation Facility (ESRF; Grenoble, France) and on the BW7A beamline at the European Molecular Biology Laboratory-Deutsches Elektronen Synchrotron (EMBL-DESY; Hamburg, Germany). The OXA-48 crystals provided a complete dataset to 1.9 Å resolution with maximum diffraction up to 1.6 Å and belong to space group $P2_1$ with cell parameters a = 63.70 Å; b = 107.18 Å; c = 80.79 Å; β = 111.04°. The crystal asymmetric unit contains four molecules and 48.3% solvent (Matthews coefficient 2.38 $Å^3$/Da). Additional details are provided as Supplemental Data.

Computational Studies

Starting coordinates for OXA-13:meropenem complex were derived from the crystal structure (1H8Y) in which the Lys-70 residue was manually carbamylated. In the case of OXA-48, a docking simulation was performed with MacroModel (Schrodinger Inc., Portland, OR) to assess the inhibitor orientation. MD and postdynamic analysis were performed with NAMD2 version 2.6 (Phillips et al., 2005) and VMD (Humphrey et al., 1996) software packages. Each complex was surrounded by a periodic box of TIP3P water molecules (Jorgensen et al., 1983). In the OXA-48 system, two Na^+ ions were added to guarantee neutrality. The simulations were conducted at 310 K and 1.0 atm, using periodic boundary conditions and particle-mesh Ewald (Essmann et al., 1995), in NPT ensemble. The X-ray structure of both enzymes was used in GRID calculations (Goodford, 1996; Goodford, 1985). A 3D 30 Å cubic box was constructed that comprised all the catalytic residues and all the secondary structure elements involved in binding of β-lactams, and inside which a grid was constructed using four points per angstrom along the three Cartesian coordinates. Grid maps were computed with the C3 probe and contoured at various energy levels using the program InsightII (Accelrys Software Inc., San Diego, CA) to visualize the favorable interaction areas of both enzymes. Full details are provided as Supplemental Data.

ACCESSION NUMBERS

The coordinates and structure factors of OXA-48 have been deposited into the Protein Data Bank under code 3HBR.

SUPPLEMENTAL DATA

Supplemental Data include Supplemental Experimental Procedures and three figures and can be found with this article online at http://www.cell.com/chemistry-biology/supplemental/S1074-5521(09)00143-4.

ACKNOWLEDGMENTS

Thanks are due to Laurent Poirel (Hôpital de Bicêtre, Université Paris XI, Paris) for providing the bla_{OXA-48} gene and for helpful discussion. We are grateful to Cristina Thaller (University of Rome "Tor Vergata") for providing us with the *E. coli* MCT236(DE3) strain. We also acknowledge the European Synchrotron Radiation Facility (Grenoble, France) for having provided access to the ID14-1 beamline and the European Molecular Biology Laboratory (Hamburg, Germany) for having provided access to the BW7 beamline.

Received: November 20, 2008
Revised: April 3, 2009
Accepted: April 10, 2009
Published: May 28, 2009

REFERENCES

Aktas, Z., Kayacan, C.B., Schneider, I., Can, B., Midilli, K., and Bauernfeind, A. (2008). Carbapenem-hydrolyzing oxacillinase, OXA-48, persists in *Klebsiella pneumoniae* in Istanbul, Turkey. Chemotherapy *54*, 101–106.

Bendtsen, J.D., Nielsen, H., von Heijne, G., and Brunak, S. (2004). Improved prediction of signal peptides: SignalP 3.0. J. Mol. Biol. *340*, 783–795.

Bou, G., Oliver, A., and Martinez-Beltran, J. (2000). OXA-24, a novel class D β-lactamase with carbapenemase activity in an *Acinetobacter baumannii* clinical strain. Antimicrob. Agents Chemother. *44*, 1556–1561.

Carrer, A., Poirel, L., Eraksoy, H., Cagatay, A.A., Badur, S., and Nordmann, P. (2008). Spread of OXA-48-positive carbapenem-resistant *Klebsiella pneumoniae* isolates in Istanbul, Turkey. Antimicrob. Agents Chemother. *52*, 2950–2954.

Cuzon, G., Naas, T., Bogaerts, P., Glupczynski, Y., Huang, T.D., and Nordmann, P. (2008). Plasmid-encoded carbapenem-hydrolyzing β-lactamase OXA-48 in an imipenem-susceptible *Klebsiella pneumoniae* strain from Belgium. Antimicrob. Agents Chemother. *52*, 3463–3464.

Dale, J.W., and Smith, J.T. (1976). The dimeric nature of an R-factor mediated β-lactamase. Biochem. Biophys. Res. Commun. *68*, 1000–1005.

Danel, F., Paetzel, M., Strynadka, N.C., and Page, M.G. (2001). Effect of divalent metal cations on the dimerization of OXA-10 and −14 class D β-lactamases from *Pseudomonas aeruginosa*. Biochemistry *40*, 9412–9420.

Docquier, J.D., Pantanella, F., Giuliani, F., Thaller, M.C., Amicosante, G., Galleni, M., Frere, J.M., Bush, K., and Rossolini, G.M. (2002). CAU-1, a subclass B3 metallo-β-lactamase of low substrate affinity encoded by an ortholog present in the *Caulobacter crescentus* chromosome. Antimicrob. Agents Chemother. *46*, 1823–1830.

Docquier, J.D., Lamotte-Brasseur, J., Galleni, M., Amicosante, G., Frere, J.M., and Rossolini, G.M. (2003). On functional and structural heterogeneity of VIM-type metallo-β-lactamases. J. Antimicrob. Chemother. *51*, 257–266.

Essmann, U., Perera, L., Berkowitz, M.L., Darden, T., Lee, H., and Pedresen, L.G. (1995). A smooth particle mesh Ewald method. J. Chem. Phys. *103*, 8577–8593.

Franceschini, N., Boschi, L., Pollini, S., Herman, R., Perilli, M., Galleni, M., Frere, J.M., Amicosante, G., and Rossolini, G.M. (2001). Characterization of OXA-29 from *Legionella* (*Fluoribacter*) *gormanii*: molecular class D β-lactamase with unusual properties. Antimicrob. Agents Chemother. *45*, 3509–3516.

Giuliani, F., Docquier, J.D., Riccio, M.L., Pagani, L., and Rossolini, G.M. (2005). OXA-46, a new class D β-lactamase of narrow substrate specificity encoded by a bla_{VIM-1}-containing integron from a *Pseudomonas aeruginosa* clinical isolate. Antimicrob. Agents Chemother. *49*, 1973–1980.

Golemi, D., Maveyraud, L., Vakulenko, S., Samama, J.P., and Mobashery, S. (2001). Critical involvement of a carbamylated lysine in catalytic function of class D β-lactamases. Proc. Natl. Acad. Sci. USA *98*, 14280–14285.

Goodford, P. (1996). Multivariate characterization of molecules for QSAR analysis. J. Chemometr. *10*, 107–117.

Goodford, P.J. (1985). A computational procedure for determining energetically favorable binding sites on biologically important macromolecules. J. Med. Chem. *28*, 849–857.

Gülmez, D., Woodford, N., Palepou, M.F., Mushtaq, S., Metan, G., Yakupogullari, Y., Kocagoz, S., Uzun, O., Hascelik, G., and Livermore, D.M. (2008). Carbapenem-resistant Escherichia coli and Klebsiella pneumoniae isolates from Turkey with OXA-48-like carbapenemases and outer membrane protein loss. Int. J. Antimicrob. Agents *31*, 523–526.

Humphrey, W., Dalke, A., and Schulten, K. (1996). VMD: visual molecular dynamics. J. Mol. Graph. *14*, 33–38.

Jorgensen, W.L., Chandrasekhar, J., Madura, J.D., Impey, R.W., and Klein, M.L. (1983). Comparison of simple potential functions for simulating liquid water. J. Chem. Phys. *79*, 926–935.

Li, J., Cross, J.B., Vreven, T., Meroueh, S.O., Mobashery, S., and Schlegel, H.B. (2005). Lysine carboxylation in proteins: OXA-10 beta-lactamase. Proteins *61*, 246–257.

Maveyraud, L., Golemi, D., Kotra, L.P., Tranier, S., Vakulenko, S., Mobashery, S., and Samama, J.P. (2000). Insights into class D β-lactamases are revealed by the crystal structure of the OXA10 enzyme from *Pseudomonas aeruginosa*. Structure *8*, 1289–1298.

Naas, T., and Nordmann, P. (1999). OXA-type β-lactamases. Curr. Pharm. Des. *5*, 865–879.

Paetzel, M., Danel, F., De Castro, L., Mosimann, S.C., Page, M.G., and Strynadka, N.C. (2000). Crystal structure of the class D β-lactamase OXA-10. Nat. Struct. Biol. *7*, 918–925.

Pernot, L., Frenois, F., Rybkine, T., L'Hermite, G., Petrella, S., Delettre, J., Jarlier, V., Collatz, E., and Sougakoff, W. (2001). Crystal structures of the class D β-lactamase OXA-13 in the native form and in complex with meropenem. J. Mol. Biol. *310*, 859–874.

Phillips, J.C., Braun, R., Wang, W., Gumbart, J., Tajkhorshid, E., Villa, E., Chipot, C., Skeel, R.D., Kale, L., and Schulten, K. (2005). Scalable molecular dynamics with NAMD. J. Comput. Chem. *26*, 1781–1802.

Poirel, L., Heritier, C., Tolun, V., and Nordmann, P. (2004). Emergence of oxacillinase-mediated resistance to imipenem in *Klebsiella pneumoniae*. Antimicrob. Agents Chemother. *48*, 15–22.

Poirel, L., Pitout, J.D., and Nordmann, P. (2007). Carbapenemases: molecular diversity and clinical consequences. Future Microbiol. *2*, 501–512.

Queenan, A.M., and Bush, K. (2007). Carbapenemases: the versatile β-lactamases. Clin. Microbiol. Rev. *20*, 440–458.

Santillana, E., Beceiro, A., Bou, G., and Romero, A. (2007). Crystal structure of the carbapenemase OXA-24 reveals insights into the mechanism of carbapenem hydrolysis. Proc. Natl. Acad. Sci. U.S.A. *104*, 5354–5359.

Sun, T., Nukaga, M., Mayama, K., Braswell, E.H., and Knox, J.R. (2003). Comparison of β-lactamases of classes A and D: 1.5-A crystallographic structure of the class D OXA-1 oxacillinase. Protein Sci. *12*, 82–91.

Voha, C., Docquier, J.D., Rossolini, G.M., and Fosse, T. (2006). Genetic and biochemical characterization of FUS-1 (OXA-85), a narrow-spectrum class D β-lactamase from *Fusobacterium nucleatum* subsp. *polymorphum*. Antimicrob. Agents Chemother. *50*, 2673–2679.

Walther-Rasmussen, J., and Hoiby, N. (2006). OXA-type carbapenemases. J. Antimicrob. Chemother. *57*, 373–383.